

# 3D Intraoral Scanner based on Piezo Laser Mechanism with Digital Image Processing

*P.S. Nethravathi, Head, MCA, Shree Devi Institute of Technology, Mangaluru, Karnataka, India.*

*G. Vidya Bai\*, Associate Professor, Department of Commerce, Manipal Academy of Higher Education, Manipal, Karnataka, India.*

*K.E. Prakash, Director, Shree Devi Institute of Technology, Mangaluru, India.*

*Gopalakrishna Bhat Kakunje, Kakunje Software Private Limited, Mangaluru, Karnataka, India.*

**Abstract**--- Based on structured illumination a three-dimensional (3D) dental scanning apparatus has been illustrated. For tuning focus, a liquid lens was used and for the shift of structured light, a piezomotor stage was used. To perform optical sectioning with structured illumination a simple algorithm, which detects intensity modulation, was used. We recreated a 3D point cloud, which represents the 3D coordinates of the digitized surface of a dental gypsum cast by piling up sectioned images. To demonstrate a 3D model of the dental cast we executed 3D registration of an individual 3D point cloud was created, which includes alignment and merging the 3D point clouds

**Keywords**--- 3D Intraoral Scanner, Structured Illumination, Liquid Lens, 3D Point Cloud.

## I. Introduction

A 3D dental scanning apparatus is illustrated based on structured illumination, for which we put a simple algorithm for 3D reconstruction. In addition, we executed 3D registration of the 3D point cloud models of each scanning point to build a 3D model of the dental gypsum cast. We developed a fast and compact 3D scanning apparatus with a liquid tunable lens and piezomotor stage. The elapsed time for a full scan was approximately 190 s, and the physical dimensions of the apparatus were 275 mm × 176 mm × 72 mm. With this 3D scanning apparatus, we rebuilt 3D point cloud models of a dental gypsum cast. The axial resolution of the 3D point cloud models was 100 μm, which coincides to the axial step of the tuning of the working distance of the 3D scanning apparatus. The accuracy of a commercial 3D intraoral scanner, which is based on the stereovision technique (Cerec Omnicam, Dentsply Sirona, York, PA, USA), was reported to be 149 μm. The accuracy of a commercial intraoral scanner which is based on structured illumination (Trios 3, 3shape) was not reported officially yet. At present, the scanning speed for our 3D scanning apparatus is restricted by the sensitivity and speed of the CMOS camera. It is likely to make the scanning faster with more sensitive and faster custom-built CMOS sensors. For the scanning speed of the commercial 3D intraoral scanners, it took 4:18 minutes to scan a full arch for Cerec Omnicam and 30 s for Trios 3. Nevertheless, Trios 3 used a CMOS sensor of 3000 frames per second and at present is the most expensive intraoral scanner.

### *Structure*

Figure 1a shows a schematic of the 3D scanning apparatus. With the exception of the mirror tip (M), the experimental setup was sealed with a housing to block external noise (Figure 1b). The dimensions of the 3D scanning apparatus were 275 mm × 176 mm × 72 mm. As an illumination source collimated white light from a light emitting diode (LED) (MCEP-CW8-070-3, Moritex, Saitama, Japan) is used. To select the vertically polarized component of the illumination source a linear polarizer was used. The collimated beam was illuminated to a Ronchi ruling (1" × 1" (20 lp/mm), Ronchi Ruling #58-777, Edmund Optics, Barrington, NJ, USA) of 50 μm periodicity. The distance between the imaging lens and the camera was the same as the distance between the imaging lens and the Ronchi ruling. The structured light was reflected off a polarization beam splitter (PBS) and traversed through an imaging lens (L) ( $f = 50$  mm), a tunable lens (TL) (EL-10-30-C, Optotune AG), and a long working distance objective lens (OBJ, working distance: 55 mm). The structured light was projected onto the sample surface and the overlapped images of the structured light and the sample were recorded by a CMOS (Complementary metal-oxide-semiconductor) camera (frame rate: 170 fps, MQ022MG-CM, Ximea, Münster, Germany). It is observable that the cross polarization detection method was used to remove internal reflection from the beam splitter and to strengthen the contrast ratio of the recorded images. We used a focus tunable lens, rather than a combination of a solid lens and a mechanical actuator, to alter the focus of the objective lens along the direction parallel to the optical axis. The tunable lens was able to tune the working distance of the objective lens from 30 to 130 mm by applying a current of 0 to 250 mA in increments of 2.5 mA.

We verified the linearity and the axial step of tuning of the working distance by imaging a depth-of-field target (Depth of Field Target 5-15 #54-440, Edmund Optics). The axial step of the tuning of the working distance was 100  $\mu\text{m}$ . It was advantageous that the focus of the tunable lens could be quickly tuned, within a few milliseconds. For each focal length, we took three consecutive images of the sample by translating the Ronchi ruling along the direction perpendicular to the optical axis. The Ronchi ruling was translated by the piezo stage (Q-522, Physik Instrumente, Karlsruhe, Germany) in steps of  $(50/3) \mu\text{m}$  across  $(100/3) \mu\text{m}$ . We recorded 300 images for the reconstruction of the 3D models at a single position. A gypsum dental cast sample (gypsum teeth model) was used for the reconstruction of the 3D point cloud model and 3D registration of the individual point cloud models. For the improved quantification of the overlapped region of the adjacent scanning area, we rearranged the gypsum dental cast along a straight line. At present, the scanning speed ( $\sim 1.9 \text{ s}$ ) for our 3D scanning apparatus is insufficient for hand-held operation, because it is restricted by the sensitivity and speed of the CMOS camera. The sample was fixed firmly on a linear motorized translation stage (M-ILS200CC, Newport, Irvine, CA, USA) and was translated in steps of 0.5 mm for each scan over a distance of 50 mm.

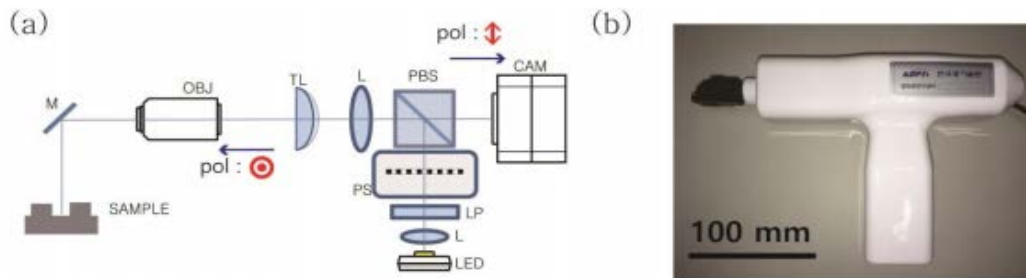


Figure 1: (a) Picture of the exploratory setup. The structured light pattern, which was created by a Ronchi ruling, focused on the sample. The scattered light from the sample was accumulated by an objective lens and recorded by a camera. The and arrow signs (red) represent the polarization of illuminated and scattered light, respectively. (M: mirror, OBJ: objective lens, TL: tunable lens, L: lens, PBS: polarizing beam splitter, CAM: camera, PS: piezo stage, LP: linear polarizer). (b) Figure of the three-dimensional scanning apparatus. The dimensions of the apparatus are 275 mm  $\times$  176 mm  $\times$  72 mm. Scale bar: 100 mm.

Figure 1b shows a depiction of the gypsum dental cast and the scanning process for the reconstruction of a 3D model of the entire gypsum dental cast. We took top-view images of the dental cast with varying the focal length of the objective lens from the top to the bottom of the cast (vertical scan). After the vertical scan was finished, the dental cast was interpreted in the lateral direction with a 0.5 mm step (lateral scan), and the next vertical scan was performed. Each single scan along a straight line over the entire dental cast took approximately 190s.

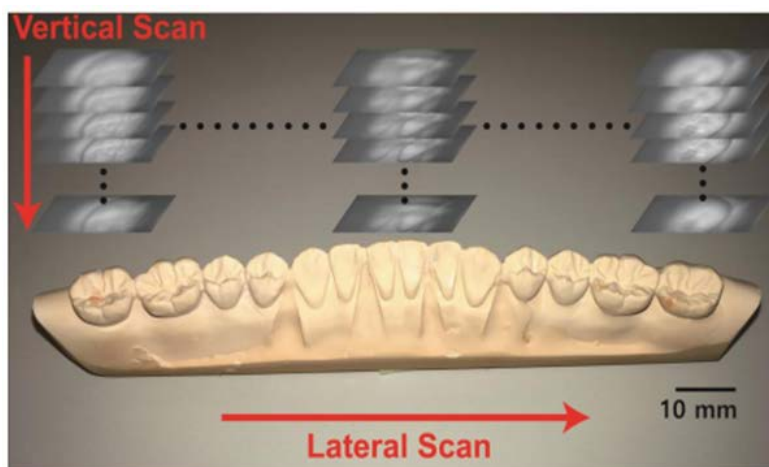


Figure 1: (b) depiction of the dental cast (gypsum model) and the images captured by the scanning apparatus from the top view. Scanning process: Images of the dental cast were listed with different objective lens focal length (vertical scan). The dental cast moved parallelly after each vertical scan was finished (lateral scan). Scale bar: 10 mm.

## II. Literature Survey

Due to its speed and non-destructiveness, non-contact optical three-dimensional (3D) shape measurement has proven to be useful for a myriad of applications, such as obstacle detection for vehicle guidance, dimensional measurement for quality inspection in automated manufacturing systems, and human body scanning. Different optical methods, including the time-of-flight method, triangulation, stereography, confocal microscopy, interferometer, and fringe projection have been developed for measuring 3D shapes.

Among the different applications, the medical applications of non-contact optical 3D shape measurement have attracted much recognition due to its benefit over conventional shape measurement techniques using custom moulds. In particular, there has been tremendous interest in the advancement of a 3D shape measurement apparatus for dental applications. The progress of a 3D intraoral scanning apparatus, which takes a digital impression of the teeth rather than a conventional impression, was one of the main parts of research aimed at dental applications. Since the introduction of digital impressions in the late 1980s, there were different commercial attempts to use an intraoral scanning apparatus for obtaining the digital impressions of the teeth.

However, there are still technical issues regarding the accuracy of the digital impressions and the scanning speed of the scanning apparatus. Recently, it was stated that a 3D intraoral scanning apparatus using optical sectioning with structured illumination provides wide-field, high-resolution images compared to other 3D intraoral scanning apparatuses. Due to the advantages of structured illumination, a 3D intraoral scanning apparatus using optical sectioning with structured illumination seems to facilitate the faster and more precise acquisition of the digital impressions.

For depth scanning, however, 3D intraoral scanning apparatuses based on structured illumination experience the mechanical movement of a focusing lens that needs additional Sensors 2017, 17, 1634; doi:10.3390/s17071634 www.mdpi.com/journal/sensors Sensors 2017, 17, 1634 2 of 9 motor-driven actuators. Recently, an electrically tunable liquid lens was used for 3D imaging, 3D microscopy, and 3D orbital tracking because of its fast response and compactness.

## III. Methodology

We carried out optical sectioning using the recorded raw images of the dental cast. Figure 4a,b is the magnified fragments of the dental cast from the same focal plane. Sinusoidal fringe patterns created by the Ronchi ruling were covered onto the raw images of the dental cast. The sinusoidal fringe patterns were only visible within the in-focus area because the Ronchi ruling and the CMOS camera were placed at the equal distance from the imaging lens. The patterns were shifted by  $T/3$  between each image, where  $T$  is the periodicity of the patterns (Figure 4c).

For the optical sectioning, instead of the phase unwrapping method, we used only the intensity of each pixel of the raw images. Sectioned images were acquired from the root-mean-square (RMS) of the sum of the squared differences between each raw image from the same focal plane. The raw images of the dental cast and its corresponding sectioned images are depicted in Figure 4d.

In the sectioned images, the white color represents the maximum-intensity of the optical sectioning and indicates a perfect in-focus state. The out-of-focus background in the sectioned images was removed by setting the upper threshold for the intensity modulation and by decoding the in-focus information. The lateral resolution of the sectioned images, which was determined by the periodicity of the sinusoidal fringe pattern, is  $50\ \mu\text{m}$ . Considering that the tunable lens and the objective lens were a single optical element, we computed the axial distance between each sectioned plane and the exit pupil of the objective lens. We recreated 3D point clouds of the teeth based on the 3D coordinates and intensity data from the optical sectioning.

## IV. Result and Analysis

The dental cast and the 3D point cloud models (polygonised surfaces) from different scanning positions. We combined sectioned images in a single volume to show various areas of the dental cast. The lateral field of view (FOV) of the 3D scanning apparatus was  $11.27\ \text{mm} \times 6\ \text{mm}$ .

In the time of the background removal process, some in-focus information was lost, which decreased the lateral area of the reconstructed 3D models. The optical sectioning depth was  $10\ \text{mm}$ , and we sliced 100 layers at an axial stepping interval of  $100\ \mu\text{m}$ . Since the axial Sensors stepping interval was much larger than the focal depth of the objective lens, the axial resolution of the 3D point cloud model and the axial stepping interval were identical.

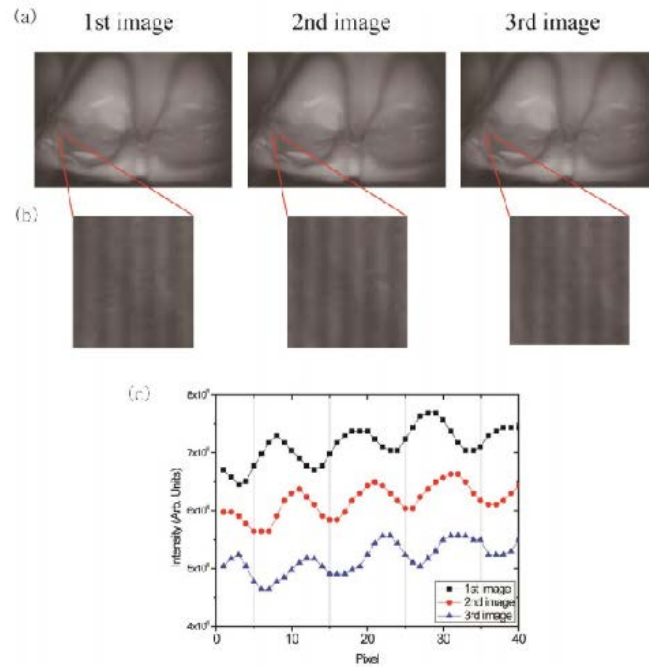


Figure 4: (a) Images (top row) of the dental gypsum cast and (b) magnified images (bottom row) of the in-focus area. Sinusoidal fringe patterns were visualized only within the in-focus areas. (c) The intensity profiles of the magnified images (Figure 4b) along the horizontal axis of the images. The intensity profiles were vertically adapted for better discrimination. The sinusoidal fringe patterns were shifted by  $T/3$  ( $T$ : periodicity of the patterns) between each image.

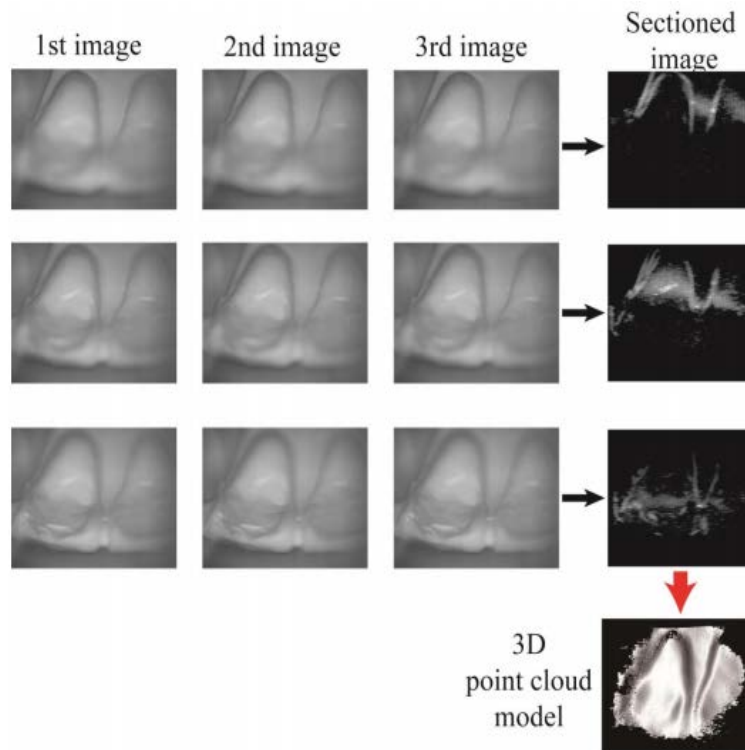


Figure 4d: Optical sectioning from the raw images of the dental cast. The intensity of each pixel of the sectioned image is defined in Equation (1). The sectioned images from different focal planes were stacked to reconstruct a 3D point cloud model of the dental cast

## V. Conclusion

In this paper, we exhibited a 3D intraoral scanning apparatus based on structured illumination. We decreased the mechanical movements of optics inside the 3D dental scanning apparatus by using a piezo stage and a liquid lens, which replaced the motor-driven actuators of conventional scanning apparatuses. Moreover, we made the scanning apparatus more compact or solid by replacing the motor-driven actuators. We recorded 2D images of the dental cast (gypsum teeth model) with changing the focus along the focal axis. For each focus, three consecutive images were captured with laterally shifting the structured illumination. We performed optical sectioning with structured illumination and reconstructed a 3D point cloud, which represents the 3D coordinates of the digitized surface, of each tooth by stacking up the sectioned images along the focal axis. In addition, we performed 3D registration (3D model aligning and stitching) of the 3D point clouds of each tooth to build a 3D model of the dental cast. We expect our results will contribute to the development of a faster and more precise 3D intraoral scanning apparatus. Moreover, our study will pave the way for further investigation of non-contact 3D shape measurements.

## References

- [1] Fachinger, J., Den Exter, M., Grambow, B., Holgersson, S., Landesman, C., Titov, M., & Podruzhina, T. (2006). Behaviour of spent HTR fuel elements in aquatic phases of repository host rock formations. *Nuclear engineering and design*, 236(5-6), 543-554.
- [2] Mettam, G. R., & Adams, L. (1999). How to prepare an electronic version of your article. *Introduction to the Electronic Age, E-Publishing Inc., New York*, 281-304.
- [3] Strunk, W., Jr., & White, E. B. (1979). *The elements of style* (3rd ed.). New York: MacMillan
- [4] Van der Geer, J., Hanraads, J.A.J., & Lupton, R. A. (2000). The art of writing a scientific article. *J. Sci. Commun*, 163(2), 51-59.